Immunobiology 224 (2019) 408–418

Contents lists available at ScienceDirect

Immunobiology

journal homepage: www.elsevier.com/locate/imbio

Full-length human surfactant protein A inhibits influenza A virus infection of A549 lung epithelial cells: A recombinant form containing neck and lectin domains promotes infectivity

Ahmed A. Al-Qahtani[a,b,1], Valarmathy Murugaiah[c,1], Hani A. Bashir[c], Ansar A. Pathan[c], Suhair M. Abozaid[a], Evgeny Makarov[c], Beatrice Nal-Rogier[c], Uday Kishore[c], Mohammed N. Al-Ahdal[a,b,*]

[a] Department of Infection and Immunity, King Faisal Specialist Hospital and Research Centre, Riyadh, Saudi Arabia
[b] Alfaisal University College of Medicine, Riyadh, Saudi Arabia
[c] Biosciences, College of Health and Life Sciences, Brunel University London, Uxbridge, UB8 3PH, United Kingdom

ARTICLE INFO

Keywords:
Innate immunity
Influenza A virus
Pulmonary collectins
Surfactant protein A

ABSTRACT

Hydrophilic lung surfactant proteins have emerged as key immunomodulators which are potent at the recognition and clearance of pulmonary pathogens. Surfactant protein A (SP-A) is a surfactant-associated innate immune molecule, which is known to interact with a variety of pathogens, and display anti-microbial effects. SP-A, being a carbohydrate pattern recognition molecule, has a wide range of innate immune functions against respiratory pathogens, including influenza A virus (IAV). Some pandemic pH1N1 strains resist neutralization by SP-A due to differences in the N-glycosylation of viral hemagglutinin (HA). Here, we provide evidence, for the first time, that a recombinant form of human SP-A (rfhSP-A), composed of α-helical neck and carbohydrate recognition domains, can actually promote the IAV replication, as observed by an upregulation of M1 expression in lung epithelial cell line, A549, when challenged with pH1N1 and H3N2 IAV subtypes. rfhSP-A (10 μg/ml) bound neuraminidase (NA) (~60 kDa), matrix protein 1 (M1) (~25 kDa) and M2 (~17 kDa) in a calcium dependent manner, as revealed by far western blotting, and direct binding ELISA. However, human full length native SP-A downregulated mRNA expression levels of M1 in A549 cells challenged with IAV subtypes. Furthermore, qPCR analysis showed that transcriptional levels of TNF-α, IL-12, IL-6, IFN-α and RANTES were enhanced following rfhSP-A treatment by both IAV subtypes at 6 h post-IAV infection of A549 lung epithelial cells. In the case of full length SP-A treatment, mRNA expression levels of TNF-α and IL-6 were downregulated during the mid-to-late stage of IAV infection of A549 cells. Multiplex cytokine/chemokine array revealed enhanced levels of both IL-6 and TNF-α due to rfhSP-A treatment in the case of both IAV subtypes tested, while no significant effect was seen in the case of IL-12. Enhancement of IAV infection of pH1N1 and H3N2 subtypes by truncated rfhSP-A, concomitant with infection inhibition by full-length SP-A, appears to suggest that a complete SP-A molecule is required for protection against IAV. This is in contrast to a recombinant form of trimeric lectin domains of human SP-D (rfhSP-D) that acts as an entry inhibitor of IAV.

1. Introduction

The initial response to an infection in a host is the activation of its innate immune system. Understanding how innate immune mechanisms restrict the spread of respiratory infections is crucial to designing therapeutic strategies. Influenza virus is a major infectious respiratory pathogen, and remains a serious global health concern, resulting in up to half a million deaths annually (WHO, 2018). There are four distinct types of Influenza virus, cause infections in humans; influenza virus A (IAV) represents the most common cause of significant health threat. IAV is responsible for approximately 70% of all influenza related deaths, and has caused highly pathogenic pandemics (WHO, 2009). IAV is further classified into different subtypes, depending on the combination of their surface glycoproteins, hemagglutinin (HA) and neuraminidase (NA) (Bouvier and Palese, 2008). IAV exerts a greater selective pressure on the host, with a complex pathogenesis, characterised

* Corresponding author.
E-mail address: profahdal@gmail.com (M.N. Al-Ahdal).
[1] AAQ and VM are joint first authors.

https://doi.org/10.1016/j.imbio.2019.02.006
Received 12 December 2018; Received in revised form 5 February 2019; Accepted 5 February 2019
Available online 11 February 2019

by rapid viral replication and viral distribution within the lungs, while evoking cellular and humoral immunity (Fukuyama and Kawaoka, 2011). Although IAV has evolved numerous molecular strategies to avoid and escape the host's immune response to promote its continuous survival within the host, a range of immune responses could potentially target any stage of IAV.

The pulmonary surfactant system is composed of abundant proteins and lipids that lower the surface tension of the alveoli, and play important roles in innate immunity. Its hydrophilic proteins, also called collectins, are soluble collagenous lectins that serve multiple antimicrobial functions against influenza viruses by binding to oligosaccharide structures via conserved carbohydrate recognition domains (CRDs) on the surface of viral particles (van de Wetering et al., 2004). The interaction between IAV and collectins (found within the mammalian serum and pulmonary fluids) leads to anti-viral activity *in vitro* (Reading et al., 1997). Bovine conglutinin and mannose binding lectin (MBL) cause inhibition of IAV hemagglutination and neutralisation (Hartley et al., 1992). Other collectins, including surfactant protein A (SP-A) and SP-D, expressed in the lungs, mucosal and epithelial surfaces in the body, are involved in a number of immune functions involving neutralization, agglutination, opsonisation and clearance of pathogens.

SP-A is a collagenous calcium-dependent defense lectins, composed of N-terminal domain rich in cysteine, collagen domain, an α-helical coiled-coil neck, and a C-terminal carbohydrate recognition domain (CRD) (Kishore et al., 2006; Nayak et al., 2012). The overall structure of SP-A is made up six of these subunits, which look like a bouquet (Kishore et al., 2006). The trimeric CRD region recognises pathogens by engaging terminal monosaccharide residues or charged patterns on microorganisms, serving as soluble pattern recognition receptors (PRRs). Thus, collagen like region is crucial for the interaction with immune cell-mediated receptors such as calreticulin-CD91 complex to bring about removal of pathogens (Kishore et al., 2006; Gardai et al., 2003).

Direct interaction between SP-A and various viruses results in viral neutralisation and induction of phagocytosis *in vitro*. SP-A can interact with glycoprotein 120 of HIV-1 and suppress infection of $CD4^+$ T cells, and enhance HIV-1 transfer via dendritic cells, serving as a dual modulator of HIV-1 infection (Gaiha et al., 2008). SP-A has also been shown to interact with herpes simplex virus type 1 (HSV-1), and mediate phagocytosis of HSV-1 by alveolar macrophages (van Iwaarden et al., 1991). SP-A can bind to the F2 subunit of respiratory syncytial virus (RSV) and neutralise its infectivity (Ghildyal et al., 1999). In the case of IAV, SP-A can bind HA and NA, and inhibit haemagglutination at initial stages. However, pH1N1 pandemic strains are not neutralised by SP-A due to variations in the N-linked glycosylation of HA (Job et al., 2010). We have recently shown a recombinant form of human surfactant protein D, containing homotrimeric neck and CRD region (rfhSP-D), binds HA and reduces M1 expression in A549 cells challenged with pH1N1 and H3N2 strains (Al-Ahdal et al., 2018). In addition, mRNA expression levels of TNF-α, IFN-α, IFN-β, IL-6 and RANTES were down-regulated following rfhSP-D treatment. Furthermore, rfhSP-D also reduced MDCK cell transduction by H1 + N1 pseudotyped lentiviral particles, suggesting a possible therapeutic potential against IAV infection. In this regards, this study was aimed at investigating the possible role of a well-characterised recombinant truncated form of human SP-A (rfhSP-A) made up of trimeric CRDs, using pH1N1 and H3N2 IAV subtypes.

2. Method and materials

2.1. Virus and antibodies

A/England/2009 (pH1N1) and the A/HK/99 (H3N2) influenza A subtypes were used for most experiments. Vesicular Stomatitis Virus (VSV-G) was used as a control for ELISA. Monoclonal Anti-Influenza Virus NA, A/California/04/2009 (pH1N1) pdm09, Clone 5C12 (produced *in vitro*), NR-42019 and A/Hong Kong/1/1968 (H3N2) (antiserum, Goat), NR-3118 and anti-M1 monoclonal antibody were obtained from BEI Resources, NIAID, NIH, USA. Monoclonal anti-influenza A virus M2 protein was obtained from Abcam.

2.2. Cell culture

Most reagents were purchased from Sigma unless mentioned otherwise. A549 and MDCK cell lines were cultured in complete DMEM containing FBS (10%), L-glutamine (2 mM), penicillin (100 U/ml), streptomycin (100 μg/ml) and sodium pyruvate (1 mM). Cells were cultured at 37 °C in a CO_2 incubator until they were 80% confluent. Cells were trypsinised (0.5%; 10 min), spun at 1000 rpm for 7′, and suspended in complete DMEM. Viable cells were counted via Trypan Blue (0.4%).

2.3. Virus purification and infection titre determination

Purification and production of pH1N1 and H3N2 subtypes were carried out as described earlier (Al-Ahdal et al., 2018). MDCK cells were infected with pH1N1 (2×10^4) or H3N2 (3.3×10^4) by incubation at 37 °C for 1 h. Post infection, the viral particles were pelleted via 3000 × g centrifugation at 4 °C for 10′. Supernatants containing virus particles were then subjected to ultracentrifugation (25,000 × g, 4 °C, 1 h 30′), followed by re-suspending virus in 100 μl of PBS. 15 μl of virus stock was assessed via reduced SDS-PAGE and ELISA. Tissue culture infectious dose ($TCID_{50}$) assay was performed to determine the infectious titre of the purified pH1N1 and H3N2 viral stocks, and to assess its cytopathic effects (CPE) using MDCK cells, as reported recently (Al-Ahdal et al., 2018). CPE effects of infected and non-infected cells were microscopically examined at each viral dilution.

2.4. Production of rfhSP-A

DNA sequences coding for trimeric neck and CRD region were cloned under T7 promoter and expressed in *Escherichia coli* BL21 (λDE3) pLysS using construct pUK-A1 (Karbani et al., 2014). *E. coli* cells were grown in LB medium, containing 100 μg/ml ampicillin and 34 μg/ml of chloramphenicol, at 37 °C until an OD_{600} reached 0.6. Following induction with 0.5 mM isopropyl β-D-thiogalactoside (IPTG), the bacterial culture was left to grow further for another 3 h on a shaker at 37 °C. The bacterial cell culture was then centrifuged (4500 rpm, 4 °C, 10′) and the pellet was re-suspended in lysis buffer (0.05 M Tris − HCL pH 7.5, 0.2 M NaCl, 0.005 M EDTA, 0.1% Triton X-100, 0.1 mM phenylmethane sulfonyl fluoride (PMSF), 50 μg lysozyme) for 1 h at 4 °C. The lysate was sonicated using a Soniprep 150 (MSE, London, UK) at 60 Hz for 30 s with an interval of 2 min (12 cycles), followed by centrifugation at 12,000 rpm for 15 min. The inclusion bodies were denatured fully in 50 ml of 0.5 M Tris − HCl, 0.1 M NaCl, pH7.5 and 8 M urea for 1 h at 4 °C. The soluble fraction was dialysed against the same buffer containing 4 M, 2 M, 1 M and no urea for 2 h at each urea concentration. The refolded material was then extensively dialysed against affinity buffer that contained 10 mM $CaCl_2$ instead of 5 mM EDTA for 2 h. The supernatant was loaded on a 5 ml of mannose-sepharose column, and bound rfhSP-A was eluted with buffer with 10 mM EDTA. Purified rfhSP-A was run on SDS-PAGE to assess its purity. LPS was removed using Endotoxin Removal Resin. LPS level was determined using QCL-1000 Limulus amebocyte lysate system (Lonza) and found to be ~5 pg/μg of rfhSP-A.

2.5. Extraction of full length native SP-A from human bronchoalveolar lavage fluid

Human full-length native SP-A (FLSP-A) was purified as published earlier (Strong et al., 1998). Bronchoalveolar lavage fluid (BAL) collected from pulmonary alveolar proteinosis patients was made up with

buffer I containing 20 mM Tris − HCl and 10 mM EDTA, pH 7.4, followed by centrifugation at 10,000 × g. The centrifuged cell pellet was extracted using buffer I with 6 M urea. The solubilised FLSP-A was centrifuged again at 10,000 × g and the soluble fraction was dialysed against 4, 2, and 1 M urea in buffer II (20 mM Tris − HCl, 100 mM NaCl, and 5 mM EDTA, pH 7.4). The supernatant was again dialysed against buffer II containing 15 mM $CaCl_2$, and loaded onto maltose agarose column, followed by elution with buffer II containing 10 mM EDTA.

2.6. SDS-PAGE

SDS-PAGE 12% (w/v) was performed to analyse and detect the purity of purified rfhSP-A and FLSP-A. Purified proteins were diluted in 1:1 (v/v) ratio in 2× Laemmli sample buffer (10 ml) (Bio-Rad, Hertfordshire) containing 1 M Tris − HCL (pH 6.8, 1 ml), 10% SDS (4 ml), 100% Glycerol (2 ml), 1% Bromophonol blue, β-mercaptoethanol (2.5 ml) and distilled water (d.H2O). The protein was then denatured for 10 min at 95 °C before loading. Standard pre-stained protein marker (Fisher Scientific) was also loaded to assess the size of the purified rfhSP-A. The SDS-PAGE gel was stained overnight using staining solution (1 g of Brilliant Blue, 50% v/v methanol, 10% acetic acid and 40 ml of D.H_2O). The stained gel was then de-stained using the de-staining solution 40% (v/v) methanol, 10% (v/v) acetic acid until the protein bands were visible.

2.7. Direct binding ELISA

FLSP-A, rfhSP-A, rfhSP-D and VSV-G (as a negative control protein) (10, 5, 2.5, and 1.25 μg/well) were coated on microtitre wells of a Maxisorp 96 well plate (Sigma-Aldrich) in carbonate/bicarbonate buffer, pH 9.6 and incubated at 4 °C overnight. After washing with PBS three times, the unoccupied sites on the wells were blocked with 2% w/v BSA for 2 h at 37 °C, followed by washing with PBST (PBS + 0.05% Tween 20). pH1N1/H3N2 virus (20 μl of 1.36×10^6 pfu/ml) was diluted 10 times using PBS, and 10 μl was incubated in the wells for 2 h at RT. After washing, monoclonal anti-H1 and polyclonal anti-H3 (both from BEI-Resources) in PBS (1:5000) were added to the appropriate wells and incubated at 37 °C for 1 h, followed by 1 h incubation with rabbit anti-mouse and protein A conjugated to HRP (1:5000), respectively (Fisher Scientific). TMB was used as a substrate and the plate was read at OD_{450}.

2.8. Far western blotting

Purified pH1N1/H3N2 (1.36×10^6pfu/ml) was run on SDS-PAGE and then separated proteins were transferred to a PVDF membrane using transfer buffer (0.25 M Tris, 0.19 M glycine and 20% methanol). After blocking the membrane with 5% w/v milk power in PBS at 4 °C and washing with PBST, the membrane was probed with monoclonal anti-NA, anti-M1 or anti-M2 (1:1000 dilutions) antibodies for 1 h at RT. For far-western blotting, the membrane was incubated with 5 μg/ml of rfhSP-A in 5 mM $CaCl_2$ buffer overnight at 4 °C. Binding was probed with rabbit anti-human SP-A polyclonal antibodies in PBS (1:1000) for 1 h at RT. Rabbit anti-mouse and Protein A conjugated to HRP (1:5000) (Fisher Scientific) were used as respective conjugates/secondary probes for monoclonal and polyclonal antibodies. The colour was developed using DAB as a substrate and H_2O_2.

2.9. Cell-binding assay

A549 cells (10,000 cells per well) were seeded in complete DMEM and incubated at 37 °C until 80% confluence was reached. After washing with different concentration of purified rfhSP-A (1.25–10 μg/ml) were pre-treated with pH1N1/H3N2 virus (1.36×10^6 pfu/ml). 10 μl of diluted virus stock was added to the appropriate wells, and incubated for 2 h at RT. After fixing the wells with 4% v/v paraformaldehyde (Fisher Scientific) for 10′ at RT, the blocking step was carried out using 2% w/v BSA. Anti-H1 and H3 antibodies and secondary probes were used, as described earlier, using TMB as a substrate.

2.10. Quantitative RT-PCR

rfhSP-A and FLSP-A (10 μg/ml) were added to A549 cells (0.5×10^6) in DMEM + 5 mM $CaCl_2$ with MOI 1 of H1N1/H3N2 virus and pelleted at different time points. Total RNA was extracted from the above-mentioned cells using GenElute Mammalian Total RNA Purification Kit (Sigma-Aldrich, UK). Total RNA was treated with DNase I (Sigma-Aldrich, UK) prior to assessing concentration and purity of total RNA via reading at OD_{260} and OD_{260}:OD_{280}(NanoDrop 2000/2000c; Thermo Fisher Scientific). 2 μg of RNA was converted into cDNA using cDNA Kit (Applied Biosystems). qRT-PCR was performed using the 7900 H T Fast Real-Time PCR System (Applied Biosciences). Each reaction was carried out in triplicates and included 5 μl Power SYBR Green MasterMix, 75 nM of FP and RP, and 500 ng cDNA. The amplification cycle involved 50 °C and 95 °C for 2′ and 10′, followed by 40 cycles of amplification. Human 18S rRNA was used to normalise gene expression and as an endogenous control. A list of primers have been provided in Table 1.

2.11. Multiplex cytokine array analysis

In order to measure the secreted cytokines and chemokines following rfhSP-A treatment, IAV treated A549 cells were incubated in the presence or absence of rfhSP-A (10 μg/ml) for 24 h. Subsequently, supernatants were collected for measuring IL-6, TNF-α, IL-8, IL12 (p40) and MCP-1. The expression levels of various analytes were measured using EMD Millipore multiplex kit. As per manufacture's instruction, 25 μl assay buffer was added to microtiter wells, plus 25 μl standard, control or supernatant of A549 cells. Magnetic beads (25 μl) linked-analytes were added to each well and incubated at 4 °C for 18 h. After assay buffer washing, detection antibodies (25 μl) were incubated with beads at RT for 1 h. 25 μl of Streptavidin-Phycoerythrin was then added to each well and incubated for 30 min. at RT. After another round of washing, 150 μl of sheath fluid was added to each well and the plate was read using the Luminex Magpix instrument.

Table 1
Target Genes, Forward and Reverse primers used for qPCR.

Target	Forward Primer	Reverse Primer
18S	5′-ATGGCCGTTCTTAGTTGGTG-3′	5′-CGCTGAGCCAGTCAGTGTAG-3′
IL-6	5′-GAAAGCAGCAAAGAGGCACT-3′	5′-TTTCACCAGGCAAGTCTCCT-3′
IL-12	5′-AACTTGCAGCTGAAGCCATT-3′	5′-GACCTGAACGCAGAATGTCA-3′
TNF-α	5′-AGCCCATGTTGTAGCAAACC-3′	5′-TGAGGTACAGGCCCTCTGAT-3′
M1	5′AAACATATGTCTGATAACGAAGGAGAACAGTTCTT-3′	5′GCTGAATTCTACCTCATGGTCTTCTTGA-3′
RANTES	5'-GCGGGTACCATGAAGATCTCTG-3'	5'-GGGTCAGAATCAAGAAACCCTC-3'
IFN-α	5'-TTT CTC CTG CCT GAA GGA CAG-3'	5'-GCT CAT GAT TTC TGC TCT GAC A-3'

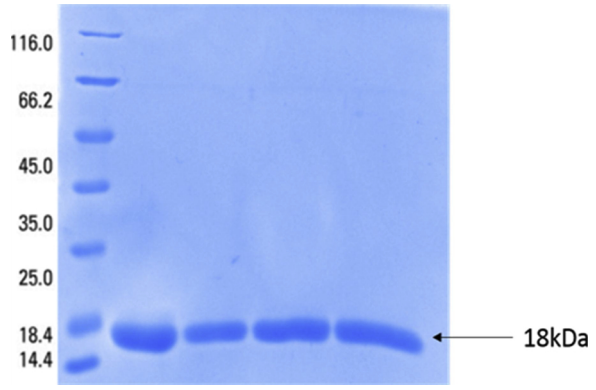

Fig. 1. SDS-PAGE (15% w/v) analysis of affinity purified recombinant fragment of Human Surfactant protein (rfhSP-A). pUK-A1 construct containing neck and CRD region was expressed under T7 bacteriophage in *Escherichia coli* BL21 (λDE3) pLysS. Following IPTG induction, the expressed bacterial cells show rfhSP-A overexpression at ~18 kDa. The inclusion bodies were refolded and affinity purified using a mannose-agarose column. Purified rfhSP-A appeared as a homogenous band of ~18 kDa.

2.12. Statistical analysis

GraphPad Prism 6.0 software was used to generate all the graphs. Two-way ANOVA test was used to perform the statistical analysis, and the significance values were considered between rfhSP-A treated and untreated conditions based on *p < 0.1, **p < 0.05, ***p < 0.01, and ****p < 0.001. Error bars show the SD or SEM (figure legends).

3. Results

3.1. Interaction of affinity purified rfhSP-A and FLSP-A with pH1N1/H3N3

The affinity purified and LPS-free rfhSP-A appeared as a single band at ~18 kDa on 15% SDS-PAGE (v/v) under reducing condition (Fig. 1). FLSP-A preparation appeared mostly as a ~32 kDa monomer, with a small proportion showing up as a non-reducible dimer of ~64 kDa (data not shown). The interaction of FLSP-A, rfhSP-A, and rfhSP-D with pH1N1/H3N2 viral particles was determined using direct binding ELISA. As shown in Fig. 2, FLSP-A, rfhSP-A and rfhSP-D bound IAV subtypes in a dose and calcium-dependent manner. No significant binding was observed with VSV-G pseudotyped lentivirus (negative control RNA virus). Cell binding assay was also performed to assess the interaction of rfhSP-A with A549 lung epithelial cells challenged with pH1N1 and H3N2 (Fig. 3). Maximum cell binding was seen at 10 µg/ml for both IAV subtypes, while a clear dose dependent binding was seen with H3N2, compared to pH1N1.

3.2. rfhSP-A interaction with NA, M1, and M2 proteins of pH1N1 and H3N2

Binding of rfhSP-A to NA (~60 kDa), M1 (~25 kDa) and M2 (~17 kDa) of purified pH1N1 and H3N2 was established using far western blotting (Fig. 4A). The ability of rfhSP-A to bind immobilised purified recombinant NA was assessed using ELISA. As shown in Fig. 4C, rfhSP-A interacted with NA dose- and calcium-dependently; VSV-G-pseudotyped particles did not show significant binding. Polymerization of M1 is suggested to provide a crucial mechanism for the elongation of filamentous IAV virions. In addition, rfhSP-A was also found to bind matrix protein 2 (M2) migrating at ~17 kDa, as evident from western blotting (Fig. 4A). Binding of rfhSP-A to M2 protein may suggest enhancement of viral replication by stabilising the viral budding site, enabling M2 polymerization leading to formation of filamentous viral particles.

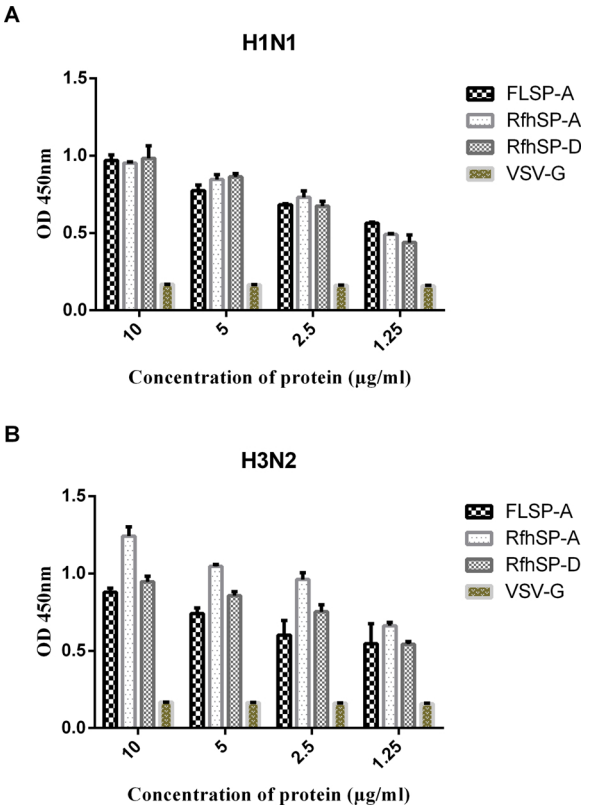

Fig. 2. Binding of rfhSP-A to (A) pH1N1 and (B) H3N2 via ELISA. Microtiter wells were coated with varied concentrations of FLSP-A, rfhSP-A and rfhSP-D (10, 5, 2.5, and 1.25 µg/ml). 20 µl of concentrated pH1N1 or H3N2 virus (1.36×10^6 pfu/ml) was diluted in 200 µl of PBS + 5 mM $CaCl_2$ and 10 µl of the diluted virus was added to all the wells, and probed with either monoclonal anti-influenza virus H1 or polyclonal anti-influenza virus H3 antibody. VSV-G pseudotyped lentivirus was used as a negative RNA virus control. The data were expressed as mean of three independent experiments done in triplicates ± SEM.

3.3. rfhSP-A promotes, while FLSP-A inhibits, infection of A549 cells by IAV

Infection assay was performed to determine the ability of IAV to infect A549 cells in the presence or absence of FLSP-A and rfhSP-A (10 µg/ml). rfhSP-A treatment up-regulated M1 expression in infected A549 cells when compared to untreated cells challenged only with virus (Fig. 5). In the case of both IAV subtypes, rfhSP-A treatment upregulated M1 expression at 2 and 6 h. The up-regulation of M1 expression was more pronounced for H3N2 than pH1N1, where $7\log_{10}$ fold up-regulation was noted at 6 h (Fig. 5A). M1 is known to bind cytoplasmic ends of HA and NA of IAV, allowing M1 association with lipid raft membrane, and inducing change in its conformation and polymerization at the site of virus budding (Gómez-Puertas et al., 2000). However, FLSP-A caused downregulation of M1 expression at 2 h and 6 h in the case of both IAV subtypes. The suppression of M1 following FLSP-A treatment was more evident in the case of pH1N1 when compared to H3N2, where -5 $\log_{10}$ fold reduction was seen at 6 h (Fig. 5B). This data is using rfhSP-A is in contrast to a recent study using rfhSP-D, where -8 $\log_{10}$ fold downregulation of M1 expression was seen with pH1N1 at 2 h (Al-Ahdal et al., 2018).

3.4. qRT-PCR analysis of modulation of immune responses by rfhSP-A on A549 challenged with IAV subtypes

The mRNA levels of pro-inflammatory cytokines and chemokines were determined via qPCR. The relative mRNA levels of TNF-α, IL-12,

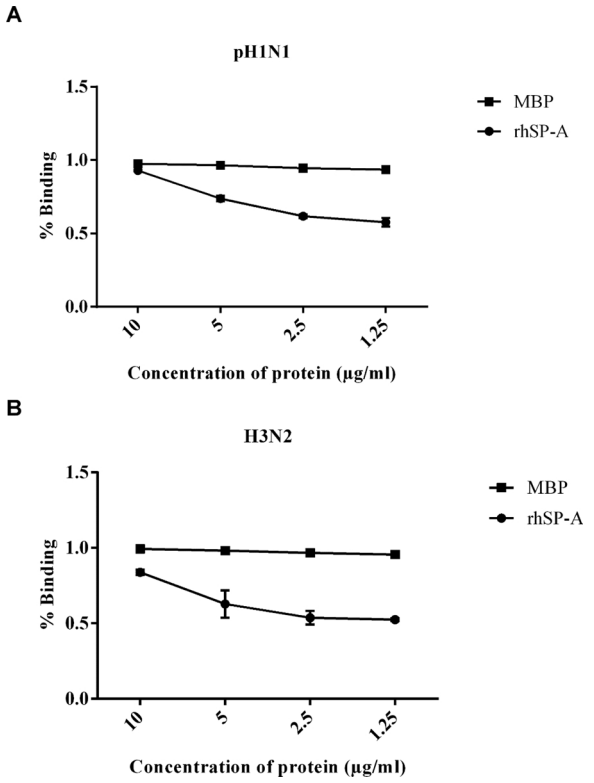

Fig. 3. Cell-binding assay to show binding of (A) pH1N1 and (B) H3N2, pre-incubated with rfhSP-A, to A549 cells. Microtiter wells were coated with A549 cells (1×10^5 cells/ml) and incubated overnight at 37 °C. Different concentrations of rfhSP-A (10, 5, 2.5, and 1.25 µg/ml), pre-incubated with pH1N1 and H3N2 virus were added to the corresponding wells, followed by incubation at room temperature for 2 h. After fixing the cells with 4% paraformaldehyde, monoclonal anti-influenza virus H1, or polyclonal anti-influenza virus H3 antibodies were added to the corresponding wells. Maltose-binding protein (MBP) was used as a negative control protein. The data were expressed as mean of three independent experiments carried out in triplicates ± SEM.

IFN-α, and RANTES were upregulated by both IAV strains, following rfhSP-A treatment at 6 h time point. However, IL-6 was $2\log_{10}$ fold upregulated by pH1N1 at 6 h by rfhSP-A treatment (Fig. 6A), but no significant change was obeserved with H3N2 strain at 6 h. Furthermore, enhancement of IFN-α was also evident with rfhSP-A treatment at 2 h, which gradually declined by $2\log_{10}$ fold at 6 h (Fig. 7A). Upregulation of type I interferon may suggest that rfhSP-A can enhance viral replication, and thus, increase the levels of interferon type I response to alert other immune cells to mobilise mechanisms towards viral clearance. In the case of FLSP-A treatment, pro-inflammatory cytokines such as TNF-α and IL-6 were downregulated at 6 h treatment for both pH1N1 and H3N2 (Fig. 6C & D). Enhanced level of IL-6 has been reported in patients infected with pH1N1 (Paquette et al., 2012). IL-12 (-2 $\log_{10}$ fold) and RANTES (-6.5 $\log_{10}$ fold) were downregulated by FLSP-A treatment in pH1N1 subtype (Fig. 6C), while this upregulation was seen with H3N2 (Fig. 6D), suggesting the possible enhancement of Th1 immune response. In the case of type I interferons, FLSP-A induced upregulation of INF-α at 6 h for both IAV strains.

3.5. Multiplex analysis of cytokine/chemokine array following rfhSP-A treatment

Secretion of cytokines and chemokines, 24 h post rfhSP-A treatment, was assessed using a multiplex cytokine/chemokine array. rfhSP-A triggered enhancement of TNF-α, IL-6 and IL-8 in both IAV subtypes (Fig. 8). However, no significant change in the level of MCP-1 was seen with MCP-1 for both IAV subtypes. Increased IL-6 level has been linked with the severity of IAV infection based on a study involving pH1N1-infected mice (Paquette et al., 2012). Expression of TNF-α in lung epithelial cells is suggested to be the key targets of IAV, and is important for controlling IAV in the host respiratory tract. TNF-α is involved in recruiting monocytes, T and B lymphocytes to the site of infection, suggesting its role in clearing the viral particles in the respiratory tract prior to the induction of secondary immune response. Therefore, up-regulation of TNF-α and IL-6 by rfhSP-A can serve as a potential biomarker during IAV infection, similar to other diseases (Damas et al., 1992; Theoharides et al., 2002).

4. Discussion

Influenza A virus (IAV) is a contagious respiratory virus, causing substantial morbidity and mortality. Anders et al. first reported collectins as beta inhibitors derived from bovine and mouse. The calcium dependent mannose binding lectin (MBL) was shown to bind glycans found on the globular region of HA, thus, inhibiting HA from binding to sialic acid-decorated cell-surface receptors (Anders et al., 1990). Collectins can orchestrate a number of anti-IAV mechanisms such as inhibition of HA and NA (Hartshorn et al., 1994, 2008; Al-Ahdal et al., 2018), virus neutralisation, virus aggregation, IAV uptake by neutrophils, and viral opsonisation. SP-A is a calcium-dependent hydrophilic C-type collectin, involved in pulmonary surfactant homeostasis (Weaver and Whitsett, 1991), and reported to be a potent innate immune molecule in the lungs. SP-A can bind various self and non-self-ligands in a calcium- dependent manner, mostly via CRD region on the target surface. Thus, recruitment and activation of immune cells occurs via collagen domain for the clearance of microorganisms (Kishore et al., 2006). SP-A can bind a diverse group of pathogens, acting as opsonins leading to direct and indirect biological consequences (Crouch, 2000; Lawson and Reid, 2000; Crouch and Wright, 2001). Specific interaction of SP-A with a number of respiratory viruses has been reported, which requires interaction with viral glycoproteins and complex oligosaccharides. Recently, we described a protective effect of rfhSP-D that was able to inhibit entry of IAV into A549 cells challenged with pH1N1 and H3N2 subtypes (Al-Ahdal et al., 2018). Therefore, this study was aimed at examining the direct interaction of a truncated recombinant fragment of human SP-A (rfhSP-A) with IAV, and subsequent immunological consequences.

In this study, plasmid pUK-A1, containing cDNA sequences for neck and CRD region of human SP-A (Karbani et al., 2014) was transformed in *Escherichia coli* BL21 (λDE3) pLysS strain under T7 bacteriophage promoter. rfhSP-A, recovered from inclusion bodies via denaturation-renaturation cycles, was affinity purified on a mannose-agarose column, which appeared as a ~18 kDa band on a 15% SDS-PAGE gel electrophoresis (Fig. 1). rfhSP-A eluted as a trimer on a gel filtration column and was recognised by rabbit polyclonal and mouse monoclonal antibodies raised against full length SP-A purified from lung lavage of an alveolar proteinosis patient (data not shown). Affinity purified rfhSP-A, made free from endotoxin, was then examined for its respective interaction with IAV subtypes (pH1N1 and H3N2) via direct ELISA (Fig. 2). The ability of rfhSP-A to bind IAV subtypes is consistent with an earlier study using a recombinant form of truncated human SP-D (rfhSP-D) composed of trimeric neck and CRD region (Al-Ahdal et al., 2018).

Ten µg/ml of rfhSP-A bound best to both pH1N1 and H3N2 (Fig. 2). The ability of rfhSP-A to bind IAV bound A549 cells was measured via cell binding assay (Fig. 3). To understand whether interaction between rfhSP-A and IAV subtypes led to specific interaction with IAV glycoproteins, far western blotting analysis was carried out (Fig. 4A). rfhSP-A (10 µg/ml) bound to NA (~60 kDa), M1 (~25 kDa) and M2 (~17 kDa) of purified pH1N1 and H3N2 in a calcium-dependent manner. Furthermore, in order to validate the binding interaction rfhSP-A and NA, an ELISA was carried out using purified recombinant NA protein. As

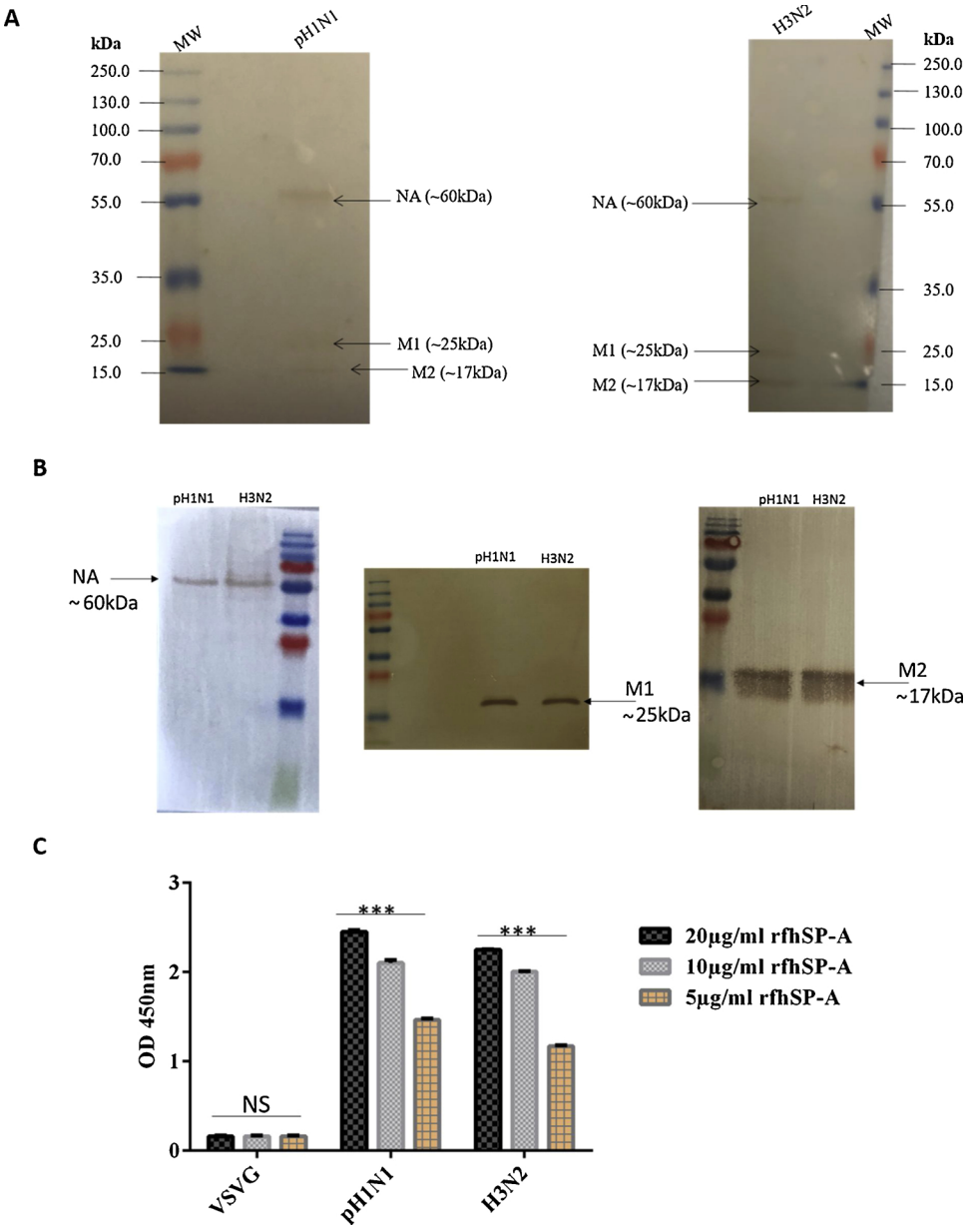

Fig. 4. (A) Far western blot analysis to show rfhSP-A binding to purified pH1N1 and H3N2. 10 µl of concentrated virus (1.36×10^6 pfu/ml) was first run on the SDS-PAGE under reducing conditions, transferred onto a nitrocellulose membrane, and incubated with 10 µg/ml of rfhSP-A. The membrane was probed with rabbit anti-human SP-A polyclonal antibody. rfhSP-A bound to NA (~60 kDa), M1 (~25 kDa) and M2 (~17 kDa) in the case of both pH1N1 and H3N2 subtypes. The identity of SP-A bound IAV proteins was validated using a separate blot that was directly probed with monoclonal anti-NA, M1 and M2 antibodies (B). (C) Direct ELISA to show the ability of rfhSP-A to bind purified recombinant neuraminidase (NA) of IAV. VSV-G was used as a negative control protein, where no significant binding was detected. The data were expressed as mean of three independent experiments carried out in triplicates ± SEM. Significance was determined using the unpaired one-way ANOVA test (***$p < 0.0001$)($n = 3$.

evident in Fig. 4B, rfhSP-A bound purified NA protein dose-dependently. Previous studies have also suggested that full length SP-A can bind to NA, and inhibit the release of viral particles from infected cells (Tecle et al., 2007). Thus, N-linked oligosaccharides found on NA are likely to be recognised by the CRD region of SP-A and SP-D (Tecle et al., 2007).

The ability of rfhSP-A to modulate viral replication and host immune response by IAV challenged A549 cells was also examined. IAV-bound rfhSP-A was found to induce enhanced viral replication, based on the expression levels of M1 gene. M1 is an abundant matrix protein of IAV, which plays dual roles in virion assembly and infection (Rossman and Lamb, 2011). Up-regulation of M1 expression was brought about by rfhSP-A treatment in IAV challenged A549 cells, compared to cells without rfhSP-A treatment but challenged with pH1N1 or H3N2 only (Fig. 5). M1 upregulation, following rfhSP-A treatment, was more pronounced in H3N2 infected cells compared to pH1N1, where 7$\log_{10}$ fold upregulation was seen at 6 h (Fig. 5). However, A549 cells, pre-treated with FLSP-A, caused downregulation of M1 expression when compared to cells only challenged with IAV subtypes (Fig. 5B). M1 downregulation by FLSP-A was found to be more effective against pH1N1 subtype, when compared to H3N2, where -5 $\log_{10}$ fold downregulation was evident at 6 h treatment (Fig. 5B). M1 can bind cytoplasmic ends of HA and NA, polymerize and form the interior structure of emerging viral particles (Rossman and Lamb, 2011). Additionally, as evident from the far western blotting, rfhSP-A was also able to bind Matrix protein 2 (M2) of IAV at ~17 kDa (Fig. 4). HA bound M1 serves as a docking site for the viral RNPs recruitment and may mediate M2 recruitment to the site of viral budding (Rossman and Lamb, 2011). M2 can stabilise the budding site, enabling polymerization of the matrix protein, leading to formation of viral particles. Furthermore, M2 has also been reported to change so as to facilitate release of the progeny viral particles. Binding of rfhSP-A to NA/M1/M2, and upregulation of M1 expression could explain the likely effect of rfhSP-A as a facilitator of IAV replication of subtypes tested in this study.

mRNA expression of pro-inflammatory cytokines and chemokines following rfhSP-A treatment was determined by qPCR, which showed an upregulation of TNF-α, IL-12 and RANTES in the case of both IAV subtypes at 6 h time point. However, an increased expression levels of IL-6 (2$\log_{10}$ fold) (Fig. 6A) was seen only with pH1N1 at 6 h, while H3N2 did not show any significant effect (Fig. 6B). In contrast,

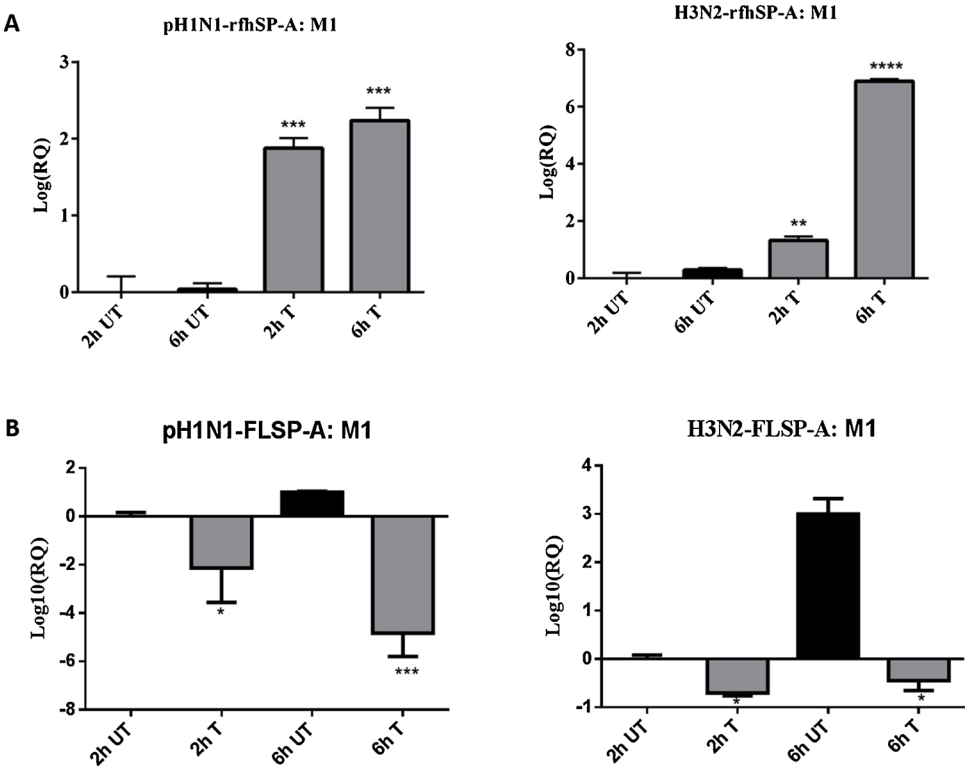

Fig. 5. rfhSP-A treatment promotes infection and replication (A), while suppression of M1 replication was seen with FLSP-A (B) of pH1N1 and (B) H3N2 in target human A549 cells. M1 mRNA expression of both pH1N1 and H3N2 influenza A virus (IAV) (MOI 1) after infection of A549 cells at 2 and 6 h was measured. A549 cells were incubated with pH1N1 and H3N2, pre-incubated with or without purified rfhSP-A and FLSP-A (10 μg/ml). Cell pellets were harvested at 2 and 6 h to analyze the M1 expression of IAV. Cells were lysed, and purified RNA extracted was converted into cDNA. Infection was measured via qRT-PCR using M1 primers; 18S was used as an endogenous control. Results shown are normalized to M1 levels at 2 h untreated. Significance was determined using the unpaired one-way ANOVA test (**$p < 0.01$, ***$p < 0.001$, and ****$p < 0.0001$) (n = 3). UT (un-treated sample), and T (treated sample).

downregulation of TNF-α (-4.5 $_{log10}$ fold) and IL-6 (-5 $_{log10}$ fold) was seen at 6 h following FLSP-A treatment (Fig. 6C & D). In the case of pH1N1, FLSP-A also caused downregulation of IL-12 and RANTES mRNA expression (Fig. 6C), while increased expression levels was observed with H3N2 IAV subtype (Fig. 6D). Enhanced levels of TNF-α and IL-6 have been reported during IAV infection, and it is also associated with severe lung pathology and worse outcome in IAV infected patients (La Gruta et al., 2007). However, these cytokines can also be protective during seasonal influenza infection. Studies also report an increased level of IL-6 in the lungs and serum of patients infected with influenza virus, including the outbreak 2009 pH1N1 pandemic subtype (Kaiser et al., 2001; Hagau et al., 2010a, 2010b). Therefore, increased levels of IL-6 following rfhSP-A treatment may be associated with facilitation of IAV infection.

Increased serum levels of TNF-α has been reported in most influenza infected patients, particularly with pH1N1 subtype (Hagau et al., 2010a, 2010b; Zúñiga et al., 2011; Bermejo-Martin et al., 2010; Morales-García et al., 2012). In this study, when pH1N1 and H3N2 were treated with rfhSP-A, TNF-α expression levels were enhanced at 6 h (Fig. 6), suggesting the ability of rfhSP-A to increase viral infection. Overexpression of TNF-α and IL-6 has been suggested as a hallmark of viral infection (Mogensen and Paludan, 2001). Elevated levels of these cytokines haven been observed in patients with both acute (Kaiser et al., 2001) and severe (Heltzer et al., 2009) seasonal IAV infection. Up-regulation of cytokine production upon H1N1 infection has been reported as an important crucial player in the pathogenesis of IAV infection. Thus, invasion of H1N1 strain into the lungs can trigger production of pro-inflammatory cytokine profile, resulting in the development of pneumonia.

rfhSP-A treatment caused increased levels of IL-12 by both pH1N1 and H3N2 in a time dependent manner (Fig. 6), suggesting the likely enhancement of viral replication and Th1 immune response. RANTES was down-regulated in the presence of rfhSP-A at 2 h, which recovered by 2.5log_{10} fold later at 6 h time point in pH1N1 treated cells. However, for H3N2, only 1log_{10} fold upregulation was seen following rfhSP-A treatment in a time-dependent manner (Fig. 6B). Lower expression levels of IFN-α was observed in the untreated sample, which was 3log_{10} fold up-regulated in the presence of rfhSP-A at 2 h (Fig. 7), suggesting that rfhSP-A can enhance the rate of viral replication, and thus, thereby enhance the levels of IFN produced by the innate immune cells in order to clear viral particles from infected host.

In conclusion, a truncated recombinant form of human SP-A, rfhSP-A, can promote pH1N1 and H3N2 subtypes of IAV instead of anticipated inhibition of infection. We have previously shown that its SP-D counterpart acts as an entry inhibitor (Al-Ahdal et al., 2018), suggesting that rfhSP-A may not have a therapeutic value. The effects of FLSP-A on IAV challenged A549 cells is similar to the effect seen by rfhSP-D, where downregulation of M1 and pro-inflammatory cytokines was seen with FLSP-A treatment. The observed restriction of M1 replication following FLSP-A treatment is likely to be due to the presence of collagen region, which could shift the way SP-A acts on IAV infectivity involving its putative receptor on the cell surface (Gardai et al., 2003). This study highlights a fundamental difference in the structure-function relationships between SP-A and SP-D. The literature is full of evidences where a recombinant truncated form of human SP-D (rfhSP-D) containing trimeric neck and CRD regions behaves like full-length SP-D *in vitro*, *in vivo* and *ex vivo*, including offering a protective effect against IAV (Madan et al., 2010; Al-Ahdal et al., 2018). In the case of SP-A and IAV interaction, it appears that only FLSP-A is capable of interfering with IAV entry into the target cells, highlighting the importance of the collagen domain and an intact SP-A molecule. It is also apparent that entry inhibition is coupled with an anti-inflammatory response, as evident from downregulation of TNF-α and IL-6. However, both FLSP-A as well as rfhSP-A upregulate type I interferon (IFN-α) response, raising the notion that FLSP-A creates an anti-inflammatory milieu during IAV infection. How rfhSP-A on its own enhances IAV infection remains an intriguing question. We are currently examining the mechanism of enhanced infectivity that may involve topological alterations in M1 and M2 proteins leading to an exaggerated budding.

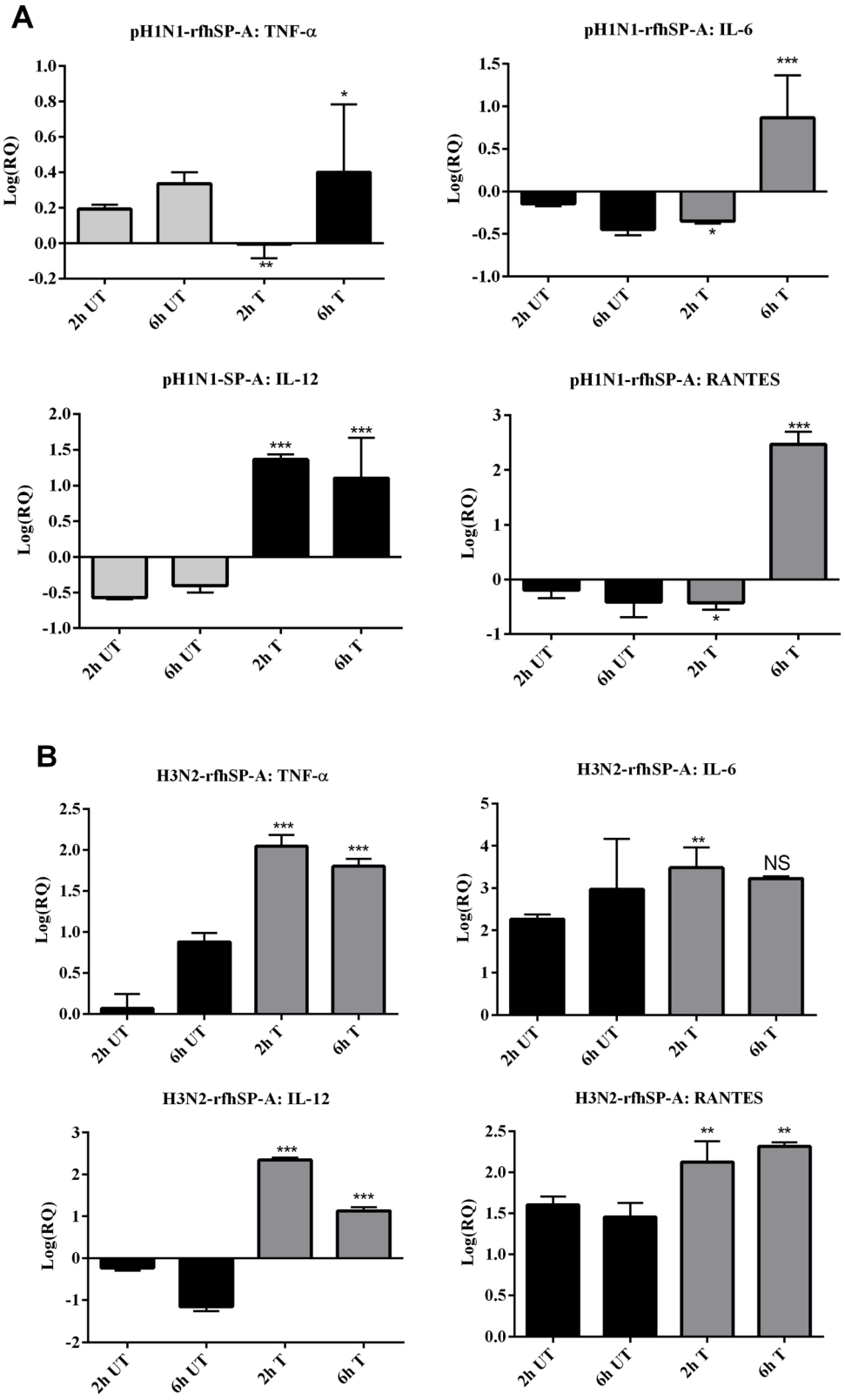

Fig. 6. Differential mRNA expression profile of selected cytokines/chemokines produced by A549 cells challenged with pH1N1 and H3N2 pre-incubated with rfhSP-A (A&B) and FLSP-A (C&D). The expression levels of selected cytokines and chemokine were measured using qRT-PCR and the data were normalized via 18S rRNA expression as a control. The relative expression (RQ) was calculated by using cells only time point as the calibrator. The RQ value was calculated using the formula: $RQ = 2-\Delta\Delta Ct$. Assays were conducted in triplicates and error bars represent ± SEM. Significance was determined using the unpaired one-way ANOVA test (**$p < 0.01$, ***$p < 0.001$, and ****$p < 0.0001$) (n = 3). UT (untreated sample), and T (treated sample).

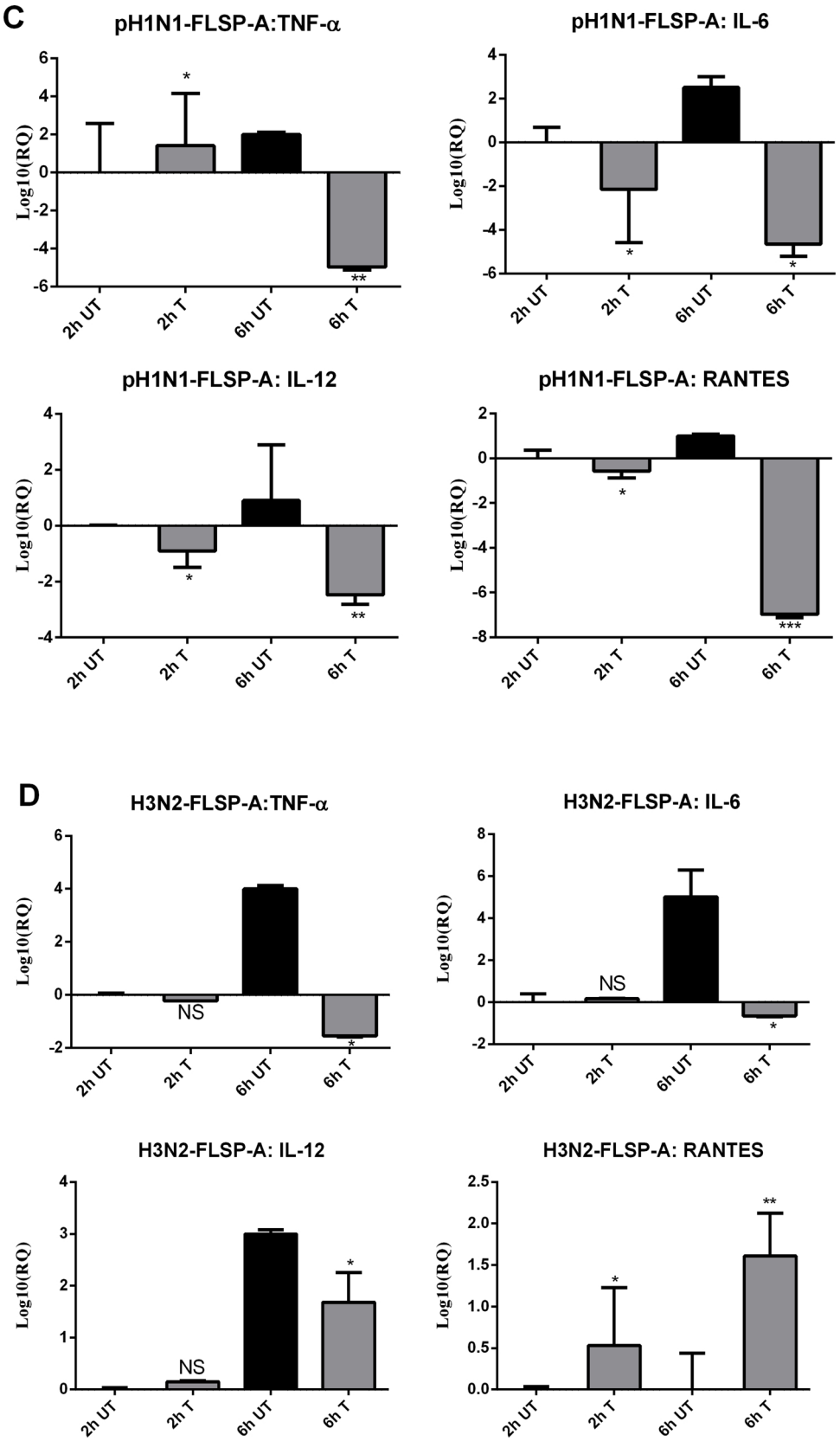

Fig. 6. (*continued*)

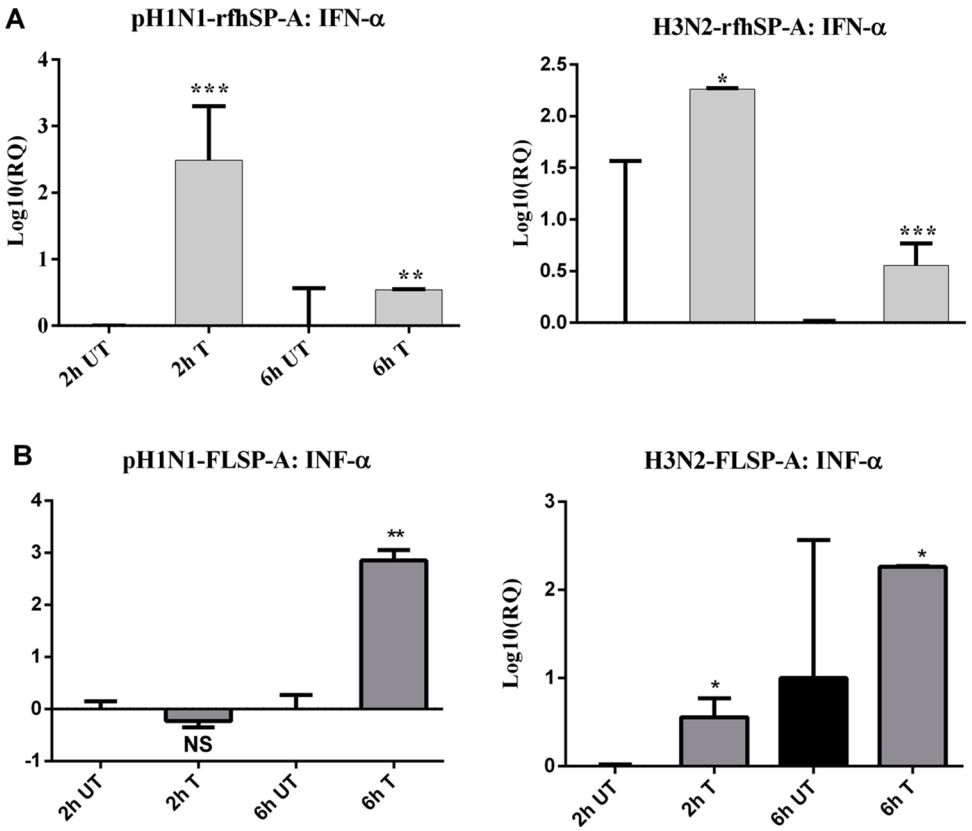

Fig. 7. mRNA expression levels of pro-inflammatory cytokine, interferon (IFN) α in untreated, rfhSP-A (A) and FLSP-A (B) treated pH1N1 and H3N2 subtype of IAV. The expression levels were measured using qRT-PCR and the data were normalized via 18S rRNA expression as an endogenous control. The relative expression (RQ) was calculated by using cells only time point as the calibrator. The RQ value was calculated using the formula: $RQ = 2-\Delta\Delta Ct$. Assays were conducted in triplicates and error bars represents ± SEM. Significance was determined using the unpaired one-way ANOVA test (*$p < 0.05$, **$p < 0.01$, ***$p < 0.001$, and ****$p < 0.0001$) (n = 3 UT (untreated sample), and T (treated sample).

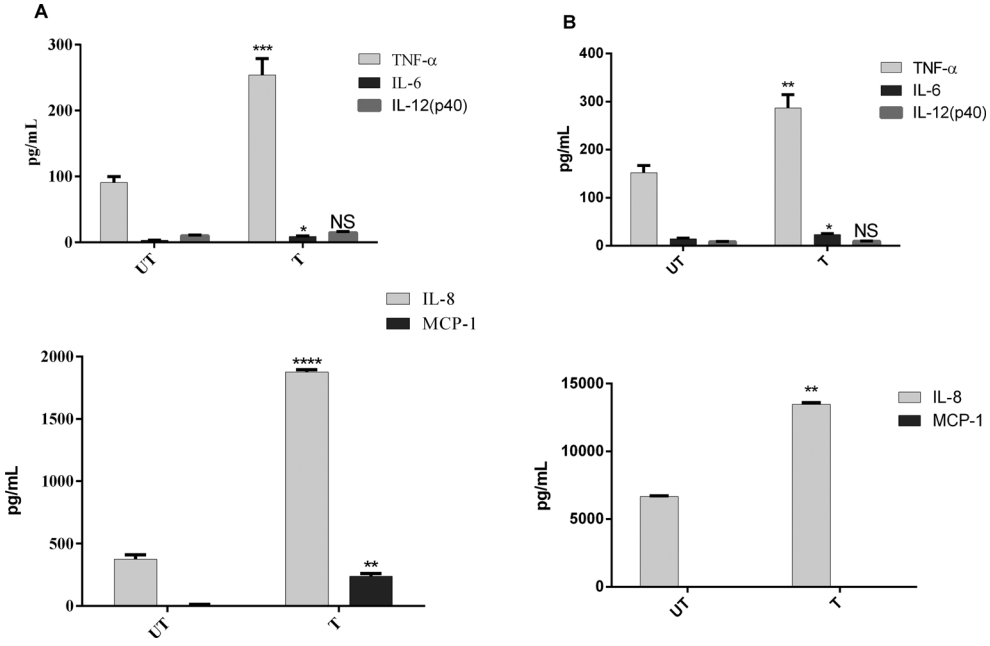

Fig. 8. Multiplex cytokine array analysis of supernatants collected at 24 h time point. A549 cells were challenged with (A) pH1N1 and (B) H3N2, followed by rfhSP-A (10 μg/ml) treatment. TNF-α, IL-6, IL-8, IL-12p40 and MCP-1 were measured using a commercially available MagPix Milliplex kit (EMD Millipore). Experiment was conducted in duplicates and error bars represent ± SEM (n = 3); significance was determined using unpaired one-way ANOVA test (*$p < 0.05$, **$p < 0.01$, ***$p < 0.001$ and ****$p < 0.0001$). UT (untreated sample), and T (treated sample).

Acknowledgements

This work was funded by the KACST (14-MED258-20) and approved by the RAC of the KFSHRC, Riyadh, Saudi Arabia (2150031). We are grateful to Maureene Delos Reyes and Hanan Shaarawi for secretarial help and administrative support. The A/England/195/2009 (pH1N1) and the A/Hong Kong/1774/99 (H3N2) strains were gifted by Wendy Barclay from the Imperial College London and Leo Poon from the University of Hong Kong, respectively. VSVG was offered by Bob Weinberg (Addgene plasmid #8454).

References

Al-Ahdal, M.N., Murugaiah, V., Varghese, P.M., Abozaid, S.M., Saba, I., Al-Qahtani, A.A., Pathan, A.A., Kouser, L., Nal, B., Kishore, U., 2018. Entry inhibition and modulation of pro-inflammatory immune response against influenza A virus by a recombinant truncated surfactant protein D. Front. Immunol. 30 (July (9)), 1586. https://doi.org/10.3389/fimmu.2018.01586. eCollection 2018.

Anders, E.M., Hartley, C.A., Jackson, D.C., 1990. Bovine and mouse serum beta inhibitors of influenza A viruses are mannose-binding lectins. Proc. Natl Acad. Sci. U. S. A. 87 (June (12)), 4485–4489.

Bermejo-Martin, J.F., Martin-Loeches, I., Rello, J., Antón, A., Almansa, R., Xu, L., Lopez-Campos, G., Pumarola, T., Ran, L., Ramirez, P., Banner, D., Ng, D.C., Socias, L., Loza,

A., Andaluz, D., Maravi, E., Gómez-Sánchez, M.J., Gordón, M., Gallegos, M.C., Fernandez, V., Aldunate, S., León, C., Merino, P., Blanco, J., Martin-Sanchez, F., Rico, L., Varillas, D., Iglesias, V., Marcos, M.Á, Gandía, F., Bobillo, F., Nogueira, B., Rojo, S., Resino, S., Castro, C., Ortiz de Lejarazu, R., Kelvin, D., 2010. Host adaptive immunity deficiency in severe pandemic influenza. Crit Care 14 (5), R167. https://doi.org/10.1186/cc9259. Epub 2010 Sep 14.

Bouvier, N.M., Palese, P., 2008. The biology of influenza viruses. Vaccine 26 (September Suppl 4), D49–53.

Crouch, E.C., 2000. Surfactant protein-D and pulmonary host defense. Respir. Res. 1 (2), 93–108 Epub 2000 Aug 25.

Crouch, E., Wright, J.R., 2001. Surfactant proteins A and D and pulmonary host defense. Annu. Rev. Physiol. 63, 521–554.

Damas, P., Ledoux, D., Nys, M., Vrindts, Y., De Groote, D., Franchimont, P., Lamy, M., 1992. Cytokine serum level during severe sepsis in human IL-6 as a marker of severity. Ann. Surg. 215 (April (4)), 356–362.

Fukuyama, S., Kawaoka, Y., 2011. The pathogenesis of influenza virus infections: the contributions of virus and host factors. Curr. Opin. Immunol. 23 (August (4)), 481–486. https://doi.org/10.1016/j.coi.2011.07.016. Epub 2011 Aug 11.

Gaiha, G.D., Dong, T., Palaniyar, N., Mitchell, D.A., Reid, K.B., Clark, H.W., 2008. Surfactant protein A binds to HIV and inhibits direct infection of CD4+ cells, but enhances dendritic cell-mediated viral transfer. J. Immunol. 181 (July (1)), 601–609.

Gardai, S.J., Xiao, Y.Q., Dickinson, M., Nick, J.A., Voelker, D.R., Greene, K.E., Henson, P.M., 2003. By binding SIRPalpha or calreticulin/CD91, lung collectins act as dual function surveillance molecules to suppress or enhance inflammation. Cell 115 (October (1)), 13–23.

Ghildyal, R., Hartley, C., Varrasso, A., Meanger, J., Voelker, D.R., Anders, E.M., Mills, J., 1999. Surfactant protein A binds to the fusion glycoprotein of respiratory syncytial virus and neutralizes virion infectivity. J. Infect. Dis. 180 (December (6)), 2009–2013.

Gómez-Puertas, P., Albo, C., Pérez-Pastrana, E., Vivo, A., Portela, A., 2000. Influenza virus matrix protein is the major driving force in virus budding. J. Virol. 74 (December (24)), 11538–11547.

Hagau, N., Slavcovici, A., Gonganau, D.N., Oltean, S., Dirzu, D.S., Brezoszki, E.S., Maxim, M., Ciuce, C., Mlesnite, M., Gavrus, R.L., Laslo, C., Hagau, R., Petrescu, M., Studnicska, D.M., 2010a. Clinical aspects and cytokine response in severe H1N1 influenza A virus infection. Crit Care 14 (6), R203. https://doi.org/10.1186/cc9324. Epub 2010 Nov 9.

Hagau, N., Slavcovici, A., Gonganau, D.N., Oltean, S., Dirzu, D.S., Brezoszki, E.S., Maxim, M., Ciuce, C., Mlesnite, M., Gavrus, R.L., Laslo, C., Hagau, R., Petrescu, M., Studnicska, D.M., 2010b. Clinical aspects and cytokine response in severe H1N1 influenza A virus infection. Crit. Care 14 (6), R203. https://doi.org/10.1186/cc9324. Epub 2010 Nov 9.

Hartley, C.A., Jackson, D.C., Anders, E.M., 1992. Two distinct serum mannose-binding lectins function as beta inhibitors of influenza virus: identification of bovine serum beta inhibitor as conglutinin. J. Virol. 66 (July (7)), 4358–4363.

Hartshorn, K.L., Crouch, E.C., White, M.R., Eggleton, P., Tauber, A.I., Chang, D., et al., 1994. Evidence for a protective role of pulmonary surfactant protein D (SPD) against influenza A viruses. J. Clin. Invest. 94, 311–319. https://doi.org/10.1172/JCI117323.

Hartshorn, K.L., Webby, R., White, M.R., Tecle, T., Pan, C., Boucher, S., et al., 2008. Role of viral hemagglutinin glycosylation in anti-influenza activities of recombinant surfactant protein D. Respir. Res. 9https://doi.org/10.1186/ 1465-9921-9-655. 65–9921–9–65.

Heltzer, M.L., Coffin, S.E., Maurer, K., Bagashev, A., Zhang, Z., Orange, J.S., Sullivan, K.E., 2009. Immune dysregulation in severe influenza. J. Leukoc. Biol. 85 (June (6)), 1036–1043. https://doi.org/10.1189/jlb.1108710.

Job, E.R., Deng, Y.M., Tate, M.D., Bottazzi, B., Crouch, E.C., Dean, M.M., Mantovani, A., Brooks, A.G., Reading, P.C., 2010. Pandemic H1N1 influenza A viruses are resistant to the antiviral activities of innate immune proteins of the collectin and pentraxin superfamilies. J. Immunol. 185 (October (7)), 4284–4291. https://doi.org/10.4049/jimmunol.1001613. Epub 2010 Sep 3.

Kaiser, L., Fritz, R.S., Straus, S.E., Gubareva, L., Hayden, F.G., 2001. Symptom pathogenesis during acute influenza: interleukin-6 and other cytokine responses. J. Med. Virol. 64 (July (3)), 262–268.

Karbani, N., Dodagatta-Marri, E., Qaseem, A.S., Madhukaran, P., Waters, P., Tsolaki, A.G., Madan, T., Kishore, U., 2014. Purification of native surfactant protein SP-A from pooled amniotic fluid and bronchoalveolar lavage. Methods Mol. Biol. 1100, 257–272. https://doi.org/10.1007/978-1-62703-724-2_21.

Kishore, U., Greenhough, T.J., Waters, P., Shrive, A.K., Ghai, R., Kamran, M.F., Bernal, A.L., Reid, K.B., Madan, T., Chakraborty, T., 2006. Surfactant proteins SP-A and SP-D: structure, function and receptors. Mol. Immunol. 43 (March (9)), 1293–1315 Epub 2005 Oct 5.

La Gruta, N.L., Kedzierska, K., Stambas, J., Doherty, P.C., 2007. A question of self-preservation: immunopathology in influenza virus infection. Immunol. Cell Biol. 85 (February-March (2)), 85–92 Epub 2007 Jan 9.

Lawson, P.R., Reid, K.B., 2000. The roles of surfactant proteins A and D in innate immunity. Immunol. Rev. 173 (February), 66–78.

Madan, T., Reid, K.B., Clark, H., Singh, M., Nayak, A., Sarma, P.U., Hawgood, S., Kishore, U., 2010. Susceptibility of mice genetically deficient in SP-A or SP-D gene to invasive pulmonary aspergillosis. Mol. Immunol. 47 (June (10)), 1923–1930. https://doi.org/10.1016/j.molimm.2010.02.027.

Morales-García, G., Falfán-Valencia, R., García-Ramírez, R.A., Camarena, Á, Ramirez-Venegas, A., Castillejos-López, M., Pérez-Rodríguez, M., González-Bonilla, C., Grajales-Muñíz, C., Borja-Aburto, V., Mejía-Aranguré, J.M., 2012. Pandemic influenza A/H1N1 virus infection and TNF, LTA, IL-1β, IL-6, IL-8, and CCL polymorphisms in Mexican population: a case-control study. BMC Infect. Dis. 13 (November 12), 299. https://doi.org/10.1186/1471-2334-12-299.

Nayak, A., Dodagatta-Marri, E., Tsolaki, A.G., Kishore, U., 2012. An insight into the diverse roles of surfactant proteins, SP-A and SP-D in innate and adaptive immunity. Front. Immunol. 7 (June (3)), 131. https://doi.org/10.3389/fimmu.2012.00131. eCollection 2012.

Paquette, S.G., Banner, D., Zhao, Z., Fang, Y., Huang, S.S., León, A.J., Ng, D.C., Almansa, R., Martin-Loeches, I., Ramirez, P., Socias, L., Loza, A., Blanco, J., Sansonetti, P., Rello, J., Andaluz, D., Shum, B., Rubino, S., de Lejarazu, R.O., Tran, D., Delogu, G., Fadda, G., Krajden, S., Rubin, B.B., Bermejo-Martin, J.F., Kelvin, A.A., Kelvin, D.J., 2012. Interleukin-6 is a potential biomarker for severe pandemic H1N1 influenza A infection. PLoS One 7 (6), e38214. https://doi.org/10.1371/journal.pone.0038214. Epub 2012 Jun 5.

Reading, P.C., Morey, L.S., Crouch, E.C., Anders, E.M., 1997. Collectin-mediated antiviral host defense of the lung: evidence from influenza virus infection of mice. J. Virol. 71 (November (11)), 8204–8212.

Rossman, J.S., Lamb, R.A., 2011. Influenza virus assembly and budding. Virology 411 (March (2)), 229–236. https://doi.org/10.1016/j.virol.2010.12.003. Epub 2011 Jan 14.

Strong, P., Kishore, U., Morgan, C., Lopez Bernal, A., Singh, M., Reid, K.B., 1998. A novel method of purifying lung surfactant proteins A and D from the lung lavage of alveolar proteinosis patients and from pooled amniotic fluid. J. Immunol. Methods 220 (November (1-2)), 139–149.

Tecle, T., White, M.R., Crouch, E.C., Hartshorn, K.L., 2007. Inhibition of influenza viral neuraminidase activity by collectins. Arch. Virol. 152 (9), 1731–1742 Epub 2007 May 22.

Theoharides, T.C., Boucher, W., Spear, K., 2002. Serum interleukin-6 reflects disease severity and osteoporosis in mastocytosis patients. Int. Arch. Allergy Immunol. 128 (August (4)), 344–350.

Van de Wetering, J.K., van Golde, L.M., Batenburg, J.J., 2004. Collectins: players of the innate immune system. Eur. J. Biochem. 271 (April (7)), 1229–1249.

Van Iwaarden, J.F., van Strijp, J.A., Ebskamp, M.J., Welmers, A.C., Verhoef, J., van Golde, L.M., 1991. Surfactant protein A is opsonin in phagocytosis of herpes simplex virus type 1 by rat alveolar macrophages. Am. J. Physiol. 261 (August (2 Pt 1)), L204–9.

Weaver, T.E., Whitsett, J.A., 1991. Function and regulation of expression of pulmonary surfactant-associated proteins. Biochem. J. 273 (January (Pt 2)), 249–264.

Zúñiga, J., Torres, M., Romo, J., Torres, D., Jiménez, L., Ramírez, G., Cruz, A., Espinosa, E., Herrera, T., Buendía, I., Ramírez-Venegas, A., González, Y., Bobadilla, K., Hernández, F., García, J., Quiñones-Falconi, F., Sada, E., Manjarrez, M.E., Cabello, C., Kawa, S., Zlotnik, A., Pardo, A., Selman, M., 2011. Inflammatory profiles in severe pneumonia associated with the pandemic influenza A/H1N1 virus isolated in Mexico city. Autoimmunity 44 (November (7)), 562–570. https://doi.org/10.3109/08916934.2011.592885.